Published in final edited form as:
J Mol Cell Cardiol. 2014 November ; 76: 106–115. doi:10.1016/j.yjmcc.2014.08.013.

Dystrobrevin increases dystrophin's binding to the dystrophin-glycoprotein complex and provides protection during cardiac stress

Jana Strakova[a], **John D. Dean**[a], **Katharine Sharpe**[a], **Tatyana A. Meyers**[a], **Guy Odom**[b], and **DeWayne Townsend**[a]

[a]Department of Integrative Biology and Physiology, University of Minnesota, Minneapolis, Minnesota, USA

[b]Department of Neurology, University of Washington, Seattle, Washington, USA

Abstract

Duchenne muscular dystrophy is a fatal progressive disease of both cardiac and skeletal muscle resulting from the mutations in the DMD gene and loss of the protein dystrophin. Alpha-dystrobrevin (α-DB) tightly associates with dystrophin but significance of this interaction within cardiac myocytes is poorly understood. In the current study the functional role of α-DB in cardiomyocytes and its implications for dystrophin function are examined. Cardiac stress testing demonstrated significant heart disease in α-DB null (adbn$^{-/-}$) mice, which displayed mortality and lesion sizes that were equivalent to those seen in the dystrophin-deficient mdx mouse. Despite normal expression and subcellular localization of dystrophin in the adbn$^{-/-}$ heart, there is a significant decrease in the strength of dystrophin's interaction with the membrane-bound dystrophin-associated glycoprotein complex (DGC). A similar weakening of the dystrophin-membrane interface was observed in mice lacking the sarcoglycan complex. Cardiomyocytes from adbn$^{-/-}$ mice were smaller and responded less to adrenergic receptor induced hypertrophy. The basal decrease in size could not be attributed to aberrant Akt activation. In addition, the organization of the microtubule network was significantly altered in adbn$^{-/-}$ cardiac myocytes, while the total expression of tubulin was unchanged in the adbn$^{-/-}$ hearts. These studies demonstrate that α-DB is a multifunctional protein that increases dystrophin's binding to the dystrophin-glycoprotein complex, and is critical for the full functionality of dystrophin.

Keywords

Alpha-dystrobrevin; dystrophin; Duchenne muscular dystrophy; tubulin

Corresponding author: DeWayne Townsend, DVM, PhD Department of Integrative Biology and Physiology University of Minnesota 1-340 CCRB 2231 6th Street SE Minneapolis, MN 55455 town0045@umn.edu Phone: +1 612 625 687.

DISCLOSURES
None

1. INTRODUCTION

Duchenne muscular dystrophy (DMD) is a devastating disease of striated muscle resulting from the deficiency in the protein dystrophin. Currently, there is no cure available for DMD patients and they eventually succumb in their second or third decade of life. Cardiomyopathy is a significant component of DMD in the majority of patients [1-4] and there is evidence that prophylactic treatment of the cardiac disease limits the dystrophic process in both skeletal and cardiac muscle [5]. Dystrophin is a large cytoskeletal protein that binds to the sarcolemma through interactions with a complex of membrane-bound glycoproteins consisting of the heterodimeric dystroglycan, the four proteins of the sarcoglycan complex, and sarcospan. This glycoprotein complex functions to serve, in part, as a link between dystrophin and the extracellular matrix [6-8]. Dystrobrevin (DB) and syntrophin are cytosolic proteins that tightly bind to dystrophin and its associated glycoproteins. Dystrobrevin was first identified in *Torpedo californica's* electric organ as a dystrophin-associated protein [9, 10]. Later, the association with dystrophin was mapped to a coiled-coil motif that is present in the C-terminal region of both proteins [11-14]. Two distinct genes encode for α- and β-DB. α-DB is predominantly expressed in the striated muscle and is alternatively spliced into several isoforms, of which α-DB-2 and -3 are the predominant forms present in the heart [15-17]. α-DB-2 localizes to the sarcolemma and, along with α-DB-1, is concentrated at neuromuscular junctions in skeletal muscle [15]. The role of the α-DB-3 isoform is unique from the longer isoforms in that it contains neither dystrophin nor syntrophin binding domains.

Although a mutation in the α-DB gene has been associated with left ventricular noncompaction [18], the precise function of α-DB in the heart remains unknown. Studies from brain and skeletal muscle demonstrate that α-DB interacts with a variety of binding partners, suggesting that it functions as a molecular scaffold for signaling molecules. Furthermore, α-DB has been shown to biochemically stabilize the dystrophin-glycoprotein complex (DGC) associations in skeletal muscle, although no functional consequence of the absence of α-DB was detected [19]. Previous studies with skeletal muscle demonstrated that α-DB is localized to the membrane via its interaction with both dystrophin and the membrane-bound sarcoglycan (SG) complex [11, 20]. Furthermore, truncated forms of dystrophin that lack the α-DB binding domain but do restore the SG complex also restore α-DB localization to the membrane [21, 22]. These data taken together provide support for physiologically relevant interaction between the SG complex and α-DB, providing a potential mechanism by which α-DB may mechanically strengthen dystrophin's interaction with the membrane [19]. α-DB has been documented to bind to a variety of other proteins including syntrophin, a signaling adapter protein that associates with many signaling proteins including neuronal nitric oxide synthase [23, 24].

In human patients with genetic disruptions of dystrophin, localization of α-DB to the membrane is significantly reduced. Similar results are obtained in patients with disruption of the SG complex [14]. In mouse models, the loss of dystrophin decreases the sarcolemma localization of α-DB isoforms 1 and 2 but the loss of sarcoglycan does not affect the localization in mice [20, 25, 26]. It is important to note that the immunofluorescent detection

of a protein near the sarcolemma does not provide information about its biochemical stability within the subsarcolemmal compartment.

The skeletal muscle phenotype of α-DB null mouse (adbn$^{-/-}$) includes abundant central nuclei, inflammatory cell infiltration, and fibrosis, although generally not as severe as that seen in the dystrophin null (mdx) mouse [27]. The functional role of α-DB in the heart is even less well understood, with mild patchy fibrosis being the only evidence of disease [27]. Here we show that the absence of α-DB results in a heart that is highly susceptible to injury during cardiac stress and provide further evidence that this susceptibility occurs secondarily to a weakening of dystrophin's interaction with the membrane-bound DGC, resulting in the significant loss of membrane integrity. The studies presented here also provide evidence that α-DB is an important modulator of cardiac myocyte hypertrophy and microtubule structure. We conclude that α-DB is an important anchor enhancing dystrophin's binding to the DGC and we propose that including the dystrobrevin binding domain will significantly improve the functionality of truncated dystrophin constructs designed for virus-mediated therapy for DMD.

2. MATERIAL AND METHODS

2.1 Animals

Control (C57BL/6J control for adbn$^{-/-}$, C57BL/10SnJ control for mdx), mdx (C57BL/10 ScSn-Dmd^{mdx}/J) and β-SG null (B6.129-Sgcbtm1Kcam/1J) mouse colonies were established at the University of Minnesota from breeding pairs obtained from Jackson Laboratories (Bar Harbor, ME, USA). Adbn$^{-/-}$ [27] maintained on C57BL/6J background mouse colonies were established from breeding pairs obtained from Dr. Jeffrey Chamberlain (University of Washington). The mice were fed standard chow diet *ad libitum* and were housed in a room with 12-hour light and dark cycles. Unless stated otherwise, mice between 4-7 months were studied. The University of Minnesota Institutional Animal Care and Use Committee approved all animal procedures.

2.2 Chronic isoproterenol stress

Wild type (C57BL/10) (n=9), adbn$^{-/-}$ (n=12) and mdx (n=12) mice received isoproterenol hydrochloride (10 mg/kg) intraperitoneally three times a day for four days and two doses on the 5th day. This isoproterenol stress test was optimized in pilot studies and the 10 mg/kg dose clearly delineated a significant survival difference between C57BL/10 and mdx mice. Animals were monitored and the time of death was recorded. Hearts were harvested, snap frozen, and processed for immunochemistry at the end point of the study, which was determined by the time of death or the end of the experimental protocol (5 days; 14 doses total). Kaplan-Meier method was used to create survival curves, followed by a Log-rank (Mantel-Cox) test to determine differences in survival (Prizm, Graph Pad, La Jolla, CA).

Similarly, a low-dose isoproterenol stress test was performed by administering 3 mg/kg of isoproterenol hydrochloride three times a day (5 days; 14 doses total) to wild type (C57BL/6) (n=4) and adbn$^{-/-}$ (n=4). At the end of the study, hearts were snap frozen and processed for immunofluorescence.

2.3 Histopathology, cell size and immunofluorescence of whole heart sections

Frozen hearts were embedded in Tissue-Tek O.C.T. Compound (Andwin Scientific, Woodland Hills, CA). Tissue blocks were cut into 7 μm-thick sections and probed with antibodies against dystrophin 1:100 (Abcam, ab15277, Cambridge, MA) and laminin 1:1000 (Sigma, L9393, St. Louis, MO) according to a standard staining protocol. Secondary antibodies (Invitrogen, Carlsbad, CA) were used to visualize dystrophin and laminin (goat anti-rabbit Alexa-488) and endogenous mouse IgG (goat anti-mouse Alexa-594). Stained sections were mounted using ProLong Gold Antifade Reagent (Invitrogen).

Images of whole heart sections were acquired on a Zeiss Axio Imager M1 microscope (Zeiss, Thornwood, NY) using AxioVision software (Zeiss) or a Nikon AZ100 Motorized Fluorescence Microscope (Nikon, Melville, NY). Measuring the levels of IgG infiltration into individual cardiomyocytes was used to assess the loss of myocardial membrane integrity. Starting in the upper left hand corner of the section non-overlapping 10x images were collected processing left to right across the section. When the right edge of the section was reached the field of view was moved vertically to begin collecting non-overlapping images right to left. This pattern was continued until the bottom of the section was reached. Only the edges of the tissue and laminin staining provided cues for image collection, the presence or absence of a lesion had no effect on which images were collected. The series of collected images included samples from the majority of the myocardial tissue. All subsequent image analysis was performed in a blinded fashion. Collected images were separated into IgG and laminin images, a threshold was set in the IgG channel that optimized the labeling of IgG positive areas. Total myocardial area was calculated using a threshold of the laminin staining that included the baseline autofluorescence. The percentage of myocardial tissue positive for IgG was calculated by dividing the number of pixels in the thresholded IgG channel by the number of pixels of myocardial tissue. This analysis was performed using ImageJ [30].

The calculation of in vivo cross-section myocyte area was performed using cardiac sections of either untreated hearts or hearts that were subjected to a low-dose, non-lethal, isoproterenol challenge. Using laminin immunofluorescence to define the edge of the myocytes, cross-sectional area was calculated using GNU Image Manipulation Program (GIMP). For the comparison of only two groups a t-test was used. Multiple comparisons used a one-way ANOVA followed by a Tukey's post-hoc analysis.

Some sections were stained with hematoxylin and eosin using standard staining procedures. Images were evaluated for evidence of myocardial injury.

2.4 Isolation of mouse cardiomyocytes

Isolation of mouse cardiomyocytes was modified from a previously published procedure [31]. Hearts were excised from animals anesthetized with sodium pentobarbital and their ascending aorta was cannulated and mounted on a perfusion aperture to allow perfusion of coronary vasculature. Hearts were perfused for 4 min with cell isolation buffer that contained (in mM): 113 NaCl, 4.7 KCl, 1.2 $MgSO_4$, 0.6 NaH_2PO_4, 0.6 KH_2PO_4 10 *2,3*-butanedione monoxime, 30 taurine, and 20 glucose. Subsequently, cell isolation buffer

containing 620 U/ml collagenase, 0.015 mg/ml DNase I, and 0.104 mg/ml protease XIV was perfused for 10 minutes. Digested hearts were triturated in the collagenase-containing buffer to free individual myocytes. Cardiomyocytes were plated on laminin-coated glass slides (Millicell EZ slide, Millipore, Millipore Billerica, MA) in M199 media (Sigma, St. Louis, MO) containing 0.02% BSA and 5% fetal bovine serum.

2.5 Primary cardiomyocytes immunofluorescence and cell size

Immunofluorescence—Freshly isolated adult mouse cardiomyocytes were fixed with 2% paraformaldehyde, blocked with 0.1 M glycine to quench free aldehyde groups, permeabilized with 0.5% Triton X-100, incubated with 1% sodium borohydrate to limit auto-fluorescence and blocked with 20% goat serum. Primary antibody against α-tubulin (1:200, Millipore, 05-829, clone DM1A) or α-actinin (1:500, Abcam, ab9465 [EA-53]) and secondary anti-mouse antibody (1:300) conjugated to Alexa Fluor-488 (Molecular Probes, Grand Island, NY, A11029) were used. Slides were mounted using ProLong Gold Antifade Reagent (Invitrogen) and imaged on a Zeiss LSM 510 Meta confocal microscope (Zeiss). To achieve uniform evaluation, the middle Z-plane of each cell was imaged with a 63x oil immersion objective and contrast and brightness were adjusted using ImageJ software [30]. Images are representative of n≥3 mice per genotype, and 10 cells were evaluated per mouse.

Cell size—C57BL/6 and adbn$^{-/-}$ derived cells were plated into 6-well tissue culture dishes and imaged on an Olympus IMT-2 (Olympus, Center Valley, PA) with 20× objective. Cell length and width was measured using Image J [30]. Each cardiomyocyte was regarded as an individual measurement for statistical analysis. A t-test was used to determine differences between the two genotypes.

2.6 Microtubule directionality

Microtubule organization was analyzed using texture detection technique (TeDT) [32]. Confocal images of cardiomyocyte α-tubulin immunofluorescence were analyzed. Analysis required selection of cellular regions that were representative of the α-tubulin staining. Selections were made as large as possible, but areas around the nucleus were avoided because they display characteristic perinuclear organization that is distinct from the sacromeric microtubule network. A two-way ANOVA was used to assess the statistical differences between the directionality histograms of C57BL/10 vs. adbn$^{-/-}$ and C57BL/10 vs. mdx.

2.7 Immunoprecipitation

Frozen hearts were pulverized and solubilized in homogenization buffer (1% Digitonin, 0.05% NP-40, 150 mM NaCl, and 50 mM Tris, pH 7.4) in the presence of proteases inhibitor cocktail (Roche Diagnostics, Indianapolis, IN) [33]. The following procedures were performed at 4°C. Homogenates were solubilized by gentle shaking for 1 h, centrifuged at 16,100xg for 99 min and the supernatant was pre-cleared with protein G agarose beads (Cell Signaling, Danvers, MA) for 1h. Protein concentration of the homogenate was adjusted (0.8 μg protein/μl) and antibody against dystrophin (Abcam, ab15277) was added. Following an overnight incubation, protein G agarose beads were added for 1 h, washed in the homogenization buffer without digitonin and proteins were

eluted by boiling with reducing sample buffer for western blot analysis. Control (data not shown) immunoprecipitations without addition of anti-dystrophin antibody or in the presence of unrelated antibody were performed to determine specificity of the interaction. Furthermore, each an immunoprecipitation reaction blot was probed for the presence of α-actinin, which was present in the homogenates but absent from the eluted fractions.

2.8 WGA assay

Dystrophin's association with the DGC was assessed by isolating glycoprotein from heart homogenates by wheat germ agglutinin (WGA) pull down, as described previously [19]. Hearts were solubilized in homogenization buffer (HB; 50 mM Tris-HCl, 500 mM NaCl, 1 mM digitonin, and protease inhibitors). Solubilized homogenates were centrifuged at 20,000xg for 20 min at 4°C and supernatant was incubated with WGA beads (Vector Laboratories, Burlingame, CA) for 2 hours at 4°C. Following several washes to remove nonbound proteins and proteins that weakly associate with glycosylated WGA-binding proteins, sample buffer was added and WGA-bound proteins were eluted by boiling. Western blot was used to quantify proteins eluted from the beads. Primary antibodies against dystrophin (Abcam, ab15277) and β-dystroglycan (Vector Laboratories, VP-13205) and secondary antibodies goat anti-mouse (Molecular Probes, A21109) and goat anti-rabbit both conjugated to Alexa Fluor-680 (Molecular Probes, A21058) were used. Fluorescent signals were scanned using Odyssey Imaging System (Li-Cor, Lincoln, Nebraska). Dystrophin's association with DGC was determined as the ratio of fluorescence intensities of dystrophin to β-dystroglycan in the same WGA-elution. A one-way ANOVA with Tukey post-test was used to determine statistical difference.

2.9 Tissue and cell homogenates

Frozen hearts were pulverized and solubilized in 1 ml of homogenization buffer that consisted of 50 mM Tris (pH 7.4), 1 mM EDTA, 588 mM KCl, 1 mM DTT, 1% Triton X-100, and protease inhibitors and incubated for 2 hours at 4°C with gently rocking. Homogenates were diluted 1:1 in homogenization buffer without KCl and centrifuged at 14,000×g for 10 min at 4°C. The supernatant was aliquoted and stored at -80 °C until analyzed.

3. RESULTS

3.1 Cardiac role of dystrobrevin revealed by chronic cardiac stress testing

Invasive cardiac catheterization of adbn$^{-/-}$ mice reveals normal hemodynamic function at baseline and following acute dobutamine administration (Supplemental Table 1). To further assess the functional cardiac reserve in adbn$^{-/-}$ mice, a chronic high-dose isoproterenol stress test (30 mg/kg/day) was performed. This five-day protocol is well tolerated by wild type mice, but both adbn$^{-/-}$ and mdx mice display significant mortality (Fig. 1). The loss of membrane integrity is a prevalent consequence of cardiac stress in the absence of dystrophin in the mdx heart [28, 34] and this isoproterenol challenge results in significant IgG infiltration into cardiomyocytes in mdx hearts. It is important to note that there are relatively low levels of myocardial injury evident in untreated mice of the ages used in the current study (Fig. 2). Interestingly, despite expressing normal levels of full-length dystrophin,

adbn$^{-/-}$ hearts display a level of injury similar to that seen in mdx hearts (Fig. 2). This data suggests that disruption of the membrane is also a fundamental feature of cardiac damage in the adbn$^{-/-}$ heart. Importantly, there is no significant post-mortem IgG infiltration observed in hearts up to 16 hours after death with the carcass kept at room temperature (data not shown), validating the utility of this assay to understand the cause of death in this survival assay. In animals that survive long enough to develop it, fibrosis and scar tissue are present in all genotypes. These changes were more prevalent in animals with longer survival times (Fig. 3A and Supplemental Fig. 1), consistent with these animals having sufficient time to develop an organized area of fibrosis. These mature lesions also display an increase in CD11b positive cells (Supplemental Fig. 2), indicating an increase in macrophage infiltration. Importantly, the isoproterenol stress testing has no effect on dystrophin localization (Fig. 3B).

3.2 Alpha-dystrobrevin significantly contributes to anchoring dystrophin to the sarcolemma, by strengthening the interaction with the DGC

Given dystrophin's proposed role as a mechanical buffer, we next investigated the strength of its association with DGC in the absence of α-DB. It is important to note that changes in whole cell β-DG, and trends for reduced dystrophin and β-SG are observed in the absence of α-DB (Fig. 4A&B), but the ratio of dystrophin to β-DG in homogenates is constant across genotypes. Wheat germ agglutinin (WGA) pull-down assays were performed to determine the ratio of dystrophin:β-DG in WGA-bound fractions as a measure of dystrophin's interaction with the membrane-bound DGC. In this assay, glycosylated proteins (such as the DGC) and proteins that tightly associate with these glycosylated proteins are pulled down, whereas weakly associated proteins are washed away. These studies demonstrate that WGA enriched membranes derived from adbn$^{-/-}$ hearts contain significantly less dystrophin relative to β-DG (30 ± 15% of control values; Fig. 4C and 4D); the remaining dystrophin is found in non-eluted fractions. Previous studies have shown that α-DB interacts with the transmembrane sarcoglycan complex [20]. We hypothesized that the sacroglycan complex would be essential for α-DB to improve the strength of dystrophin's binding to the DGC. To test this, β-SG null hearts, in which all components of the sarcoglycan complex are markedly reduced, were used to assess the role of the sacroglycan complex on dystrophin binding to the membrane-bound β-DG. Similar to adbn$^{-/-}$, WGA-enriched membranes from β-SG null hearts contain a significantly lower dystrophin:β-DG ratio (29% ± 2% of control; Fig 4C and 4D). To further assess the role of α-DB in mediating the interaction between dystrophin and the membrane-bound DGC, dystrophin was immunoprecipitated and the levels of β-DG were assessed. In wild type hearts β-DG is readily detected in the eluted fraction. In agreement with the WGA data, the levels of β-DG present in the eluted fractions from either adbn$^{-/-}$ or β-SG null hearts are almost undetectable (Fig. 4E and 4F). These data support a model where α-DB strengthens dystrophin's association with the sarcolemma by serving as a link between dystrophin and the sarcoglycan complex. Importantly, this weakened interaction between dystrophin and the membrane had no effect on the subcellular localization of dystrophin in the heart (Fig. 5A). Furthermore, visualization of the Z-disc protein α-actinin shows normal sarcomere organization in both adbn$^{-/-}$ and mdx mice (Fig. 5B) indicating that at 4-7 months of age the organization of the sarcomere is not visibly affected. Additional studies of one-year-old adbn$^{-/-}$ mice reveal very little evidence of

myocardial lesions (data not shown). This is in contrast to mdx mice, which display significant cardiac lesions by one year of age.

3.3 Abnormal cardiac size in adbn $^{-/-}$ mice

In humans, mutation in the α-DB gene has been associated with left ventricular non-compaction and congenital heart disease [18]. Morphometric analysis of adbn$^{-/-}$ hearts do not show any evidence of left ventricular non-compaction (Supplemental Fig. 3). Comparison of the heart to body weight ratio of wild type and adbn$^{-/-}$ mice reveals that the relative size of the hearts of adbn$^{-/-}$ mice is significantly smaller than that of wild type hearts (Fig. 6A). Measurements of in situ cardiomyocyte cross-sectional areas and the longitudinal areas of isolated cardiomyocytes demonstrate that adbn$^{-/-}$ derived cells are significantly smaller than myocytes from wild type hearts (Table 1 and Fig. 6B-D). Quantitative analysis of the key regulator of cardiomyocyte size, phospho-Akt (Thr308 and Ser473) does not reveal any differences in the basal state of phosphorylated (activated) Akt in untreated abdn$^{-/-}$ mice (Supplemental Fig. 4). Chronic administration of a low dose of isoproterenol (3 mg/kg) that does not cause mortality in adbn$^{-/-}$ mice results in significant levels of hypertrophy in wild type hearts, but this hypertrophic response is significantly attenuated in adbn$^{-/-}$ myocytes (Fig. 6C,D).

3.4 Microtubule network organization and density in adbn $^{-/-}$

In skeletal muscle, the absence of dystrophin results in the disorganization of the cortical microtubule network and increased tubulin expression [35-37]. While the microtubular disorder in skeletal muscle may be secondary to fiber regeneration, it is also present in the myocardium during the later stages of the disease progression [38]. Cardiomyocytes derived from older mdx mice show increased α-tubulin expression and microtubule network density [38]. We see similar results in old (>10 months) but not in adult (<7 months) mdx mice (Supplemental Fig. 5). Interestingly, analysis of α-tubulin confocal images reveals a small increase in microtubule network density in younger adbn$^{-/-}$ myocytes (Supplemental Fig. 5), suggesting that the microtubule phenotype is present earlier in adbn$^{-/-}$ myocytes compared to mdx, although strain effects complicate the interpretation of these results. Importantly, both mdx and adbn$^{-/-}$ hearts express normal levels of total α-tubulin (Supplemental Fig. 6). In wild type myocytes, longitudinally distributed α-tubulin fibers predominate the network throughout the cell. However, in adbn$^{-/-}$ and mdx myocytes there is a noticeable increase in α-tubulin fibers oriented orthogonally to the long axis of the cell (Fig. 7A). The overall organization of microtubule network was quantified by TeDT analysis [32]. This analysis confirms that mdx and adbn$^{-/-}$ cardiomyocytes contained a significant increase ($P<0.0001$) in fibers oriented orthogonally to the longitudinal axis of the cell (increase encompassed approximately 80° to 110° relative to the longitudinal axis of the cell; Fig.7B,C).

4. DISSCUSSION

The work presented here provides evidence that α-DB significantly strengthens the interaction between dystrophin and the membrane-bound DGC through its interactions with dystrophin and the sarcoglycan (SG) complex. In the absence of α-DB or the SG complex,

dystrophin is properly localized to the sarcolemmal membrane. However, our data suggest that the strength of dystrophin's binding to the DGC and thus its protective action are suboptimal. Our results show that in the absence of α-DB or the SG complex, only approximately 30% of dystrophin remains strongly bound to the membrane-bound DGC, suggesting that α-DB mechanically reinforces dystrophin's interaction with the membrane by increasing its affinity to the DGC. The residual tightly bound dystrophin likely contributes to the normal passive properties of myocytes lacking the sarcoglycan complex [39]. In adbn$^{-/-}$ mice, this residual dystrophin binding prevents skeletal muscle dysfunction [19], supports normal baseline and dobutamine-stimulated cardiac function, and limits age-related accumulation of myocardial injury. However, the significant chronic cardiac stress used in this study unveils a significant cardiomyopathy in adbn$^{-/-}$ mice resulting in severe sarcolemmal damage and an overall level of mortality comparable to mdx mice that completely lack dystrophin. We propose that the cardiac stress protocol implemented in this study creates significant long-lasting increases in cardiac contractility and that this sustained activity eventually overwhelms the weakened interaction between dystrophin and the membrane-bound DGC.

Our data supports a model where α-DB forms a bridge between dystrophin and the sarcoglycan complex. The domain through which α-DB interacts with dystrophin is a well-defined coiled-coil domain that is present in near the C-terminal of both dystrophin and α-DB [11]. There is evidence that α-DB interacts directly with solubilized the SG complex in a protein complex that includes neither dystrophin nor dystroglycan [20]. The specific domains mediating this binding are currently unknown. This study also provides experimental evidence for a potential mechanism to understand the increased functionality of μ- dystrophin constructs containing the α-DB binding domain in skeletal muscle [40]. These important studies demonstrate that inclusion of the α-DB binding domain provides more protection against lengthening-contractions than expression of constructs that cannot bind to α-DB. It is not clear if a similar improvement would be present in the heart, but these studies suggest that inclusion of this domain would provide additional strength to the binding of a μ-dystrophin construct to the DGC.

The mechanisms underlying the reduced levels of β-DG in the absence of either α-DB or β-SG are not clear. These observations are consistent with the model described above where α-DB functions to stabilize the entire DGC and this destabilized DGC is more susceptible to degradation. The decreases in the DGC components observed in the current study are somewhat surprising in the myocardium where the DGC is present at normal levels in the absence of dystrophin [29, 41-43]. These data suggest the possibility that α-DB also has a role in determining the steady-state levels of the DGC complex.

The adbn$^{-/-}$ mouse has a reduced heart to body weight ratio and significantly smaller cardiomyocytes that have an attenuated response to isoproterenol-induced hypertrophy to the same extent as the wild type cells. Akt signaling has been implicated in the regulation of both physiological and pathological forms of hypertrophy, but as demonstrated here, Akt phosphorylation under basal conditions was unchanged in the adbn$^{-/-}$ hearts. This data suggests that α-DB has a role in both developmental and induced cardiomyocyte

hypertrophy. The molecular basis by which α-DB modulates cell size remains to be elucidated.

Alteration of the microtubule network has been associated with contractile dysfunction and, at least in skeletal muscle, it is becoming clear that dystrophin plays a role. Dystrophin binds directly to microtubule filaments and in skeletal muscle the absence of dystrophin results in a disorganized network containing dense foci of polymerized tubulin [37]. Here we observe a small increase in the density of microtubule fibers in the adbn$^{-/-}$ cardiomyocytes, which is absent from young mdx. In older mdx myocytes, significant increases in tubulin density are evident, consistent with previously published work [38]. These data suggest that significant increases in microtubular density correlates with more advanced disease and that adbn$^{-/-}$ mice develop these microtubular changes earlier than in mdx myocytes. As is observed in human cardiac myocytes [44], the mouse myocytes in this study display a predominance of microtubular fibers oriented along the longitudinal axis of the cell. The pathophysiological significance of the increased levels of microtubular fibers that run perpendicular to the long axis of the cell in the dystrophic myocytes is not clear. It is important to note that the changes in microtubule organization that we report here are occurring in the middle of the cell. Therefore, any changes in network structure are unlikely to occur secondarily to direct interaction with dystrophin or α-DB, but rather result from changes that affect the entire cell. The similar change in microtubule organization in adbn$^{-/-}$ and mdx is another example of how the cardiac disease in these two genotypes overlaps, suggesting that they share the same underlying pathological mechanisms. In addition to its interaction with dystrophin, α-DB also associates with tubulin [45] in non-myocyte cells, although such interaction has not been reported in muscle cells. α-DB has also been shown to interact with several intermediate filament proteins [46, 47], the functional significance of which remains unclear.

This work has potential implications for the design of truncated dystrophins destined for use as genetic therapeutics. Virus-mediated gene therapy has the potential to restore dystrophin expression through tissue-specific introduction of genetic material. However, the size of the dystrophin transcript exceeds the capacity of the most effective viral delivery vectors and thus there is a need to create functional truncated dystrophin constructs. Dystrophin's domain structure is well characterized and several highly functional μ-dystrophins have been generated and evaluated [29, 48-51]. These studies demonstrate that these truncated dystrophins provide significant, but not complete, functional replacement of full-length dystrophin. An important feature of these constructs is that they all use a highly truncated C-terminal domain of dystrophin that does not contain the α-DB binding site [48]. There has been one study assessing the function of a C-terminally extended μ-dystrophin, which was found to be superior to prior μ-dystrophin [40]. Our study provides a potential mechanism for the functional improvement observed in this study.

5. CONCLUSION

In summary, our data indicates that α-DB is a multifunctional protein that is involved in the determination of cardiomyocyte size and potentiates dystrophin function. Given that mice expressing full-length dystrophin, but lacking α-DB, are highly susceptible to membrane

damage with cardiac stress, our data demonstrate the importance of the dystrophin-α-DB interaction for membrane protection. Furthermore, these data suggest that genetically engineered dystrophin constructs containing the α-DB binding domain may also have increased affinity for the membrane-bound DGC, which would be expected to increase the functionality of the dystrophin construct.

Supplementary Material

Refer to Web version on PubMed Central for supplementary material.

ACKNOWLEDGEMENT

The authors would like to a thank Wenhua Liu and Evelyn Ralston for their assistance with the analysis of microtubular network structure. This work was funded by grants K08 HL102066 and R01 HL114832 from the National Institutes of Health and the Greg Marzolf Jr. Foundation.

ABBREVIATIONS

abdn$^{-/-}$	alpha-dystrobrevin null mice
α-DB	alpha-dystrobrevin
β-SG	beta-Sarcoglycan

References

1. Frankel KA, Rosser RJ. The pathology of the heart in progressive muscular dystrophy: epimyocardial fibrosis. Hum Pathol. 1976; 7:375–86. [PubMed: 939536]
2. Nigro G, Comi LI, Politano L, Bain RJ. The incidence and evolution of cardiomyopathy in Duchenne muscular dystrophy. Int J Cardiol. 1990; 26:271–7. [PubMed: 2312196]
3. Politano L, Nigro V, Nigro G, Petretta VR, Passamano L, Papparella S, et al. Development of cardiomyopathy in female carriers of Duchenne and Becker muscular dystrophies. JAMA. 1996; 275:1335–8. [PubMed: 8614119]
4. Bushby K, Finkel R, Birnkrant DJ, Case LE, Clemens PR, Cripe L, et al. Diagnosis and management of Duchenne muscular dystrophy, part 1: diagnosis, and pharmacological and psychosocial management. Lancet Neurol. 2010; 9:77–93. [PubMed: 19945913]
5. Rafael-Fortney JA, Chimanji NS, Schill KE, Martin CD, Murray JD, Ganguly R, et al. Early treatment with lisinopril and spironolactone preserves cardiac and skeletal muscle in Duchenne muscular dystrophy mice. Circulation. 2011; 124:582–8. [PubMed: 21768542]
6. Crosbie RH, Heighway J, Venzke DP, Lee JC, Campbell KP. Sarcospan, the 25-kDa transmembrane component of the dystrophin-glycoprotein complex. J Biol Chem. 1997; 272:31221–4. [PubMed: 9395445]
7. Ervasti JM, Campbell KP. Membrane organization of the dystrophin glycoprotein complex. Cell. 1991; 66:1121–31. [PubMed: 1913804]
8. Ervasti JM, Campbell KP. A role for the dystrophin-glycoprotein complex as a transmembrane linker between laminin and actin. J Cell Biol. 1993; 122:809–23. [PubMed: 8349731]
9. Sadoulet-Puccio HM, Khurana TS, Cohen JB, Kunkel LM. Cloning and characterization of the human homologue of a dystrophin related phosphoprotein found at the Torpedo electric organ post-synaptic membrane. Hum Mol Genet. 1996; 5:489–96. [PubMed: 8845841]
10. Butler MH, Douville K, Murnane AA, Kramarcy NR, Cohen JB, Sealock R, et al. Association of the Mr 58,000 postsynaptic protein of electric tissue with Torpedo dystrophin and the Mr 87,000 postsynaptic protein. J Biol Chem. 1992; 267:6213–8. [PubMed: 1556129]

11. Sadoulet-Puccio HM, Rajala M, Kunkel LM. Dystrobrevin and dystrophin: an interaction through coiled-coil motifs. Proc Natl Acad Sci U S A. 1997; 94:12413–8. [PubMed: 9356463]
12. Suzuki A, Yoshida M, Hayashi K, Mizuno Y, Hagiwara Y, Ozawa E. Molecular organization at the glycoprotein-complex-binding site of dystrophin. Three dystrophin-associated proteins bind directly to the carboxy-terminal portion of dystrophin. Eur J Biochem. 1994; 220:283–92. [PubMed: 8125086]
13. Yoshida M, Yamamoto H, Noguchi S, Mizuno Y, Hagiwara Y, Ozawa E. Dystrophin-associated protein A0 is a homologue of the Torpedo 87K protein. Febs Lett. 1995; 367:311–4. [PubMed: 7607329]
14. Metzinger L, Blake DJ, Squier MV, Anderson LV, Deconinck AE, Nawrotzki R, et al. Dystrobrevin deficiency at the sarcolemma of patients with muscular dystrophy. Hum Mol Genet. 1997; 6:1185–91. [PubMed: 9215691]
15. Blake DJ, Nawrotzki R, Peters MF, Froehner SC, Davies KE. Isoform diversity of dystrobrevin, the murine 87-kDa postsynaptic protein. J Biol Chem. 1996; 271:7802–10. [PubMed: 8631824]
16. Bohm SV, Constantinou P, Tan S, Jin H, Roberts RG. Profound human/mouse differences in alpha-dystrobrevin isoforms: a novel syntrophin-binding site and promoter missing in mouse and rat. BMC Biol. 2009; 7:85. [PubMed: 19961569]
17. Enigk RE, Maimone MM. Differential expression and developmental regulation of a novel alpha-dystrobrevin isoform in muscle. Gene. 1999; 238:479–88. [PubMed: 10570976]
18. Ichida F, Tsubata S, Bowles KR, Haneda N, Uese K, Miyawaki T, et al. Novel gene mutations in patients with left ventricular noncompaction or Barth syndrome. Circulation. 2001; 103:1256–63. [PubMed: 11238270]
19. Bunnell TM, Jaeger MA, Fitzsimons DP, Prins KW, Ervasti JM. Destabilization of the dystrophin-glycoprotein complex without functional deficits in alpha-dystrobrevin null muscle. PLoS One. 2008; 3:e2604. [PubMed: 18596960]
20. Yoshida M, Hama H, Ishikawa-Sakurai M, Imamura M, Mizuno Y, Araishi K, et al. Biochemical evidence for association of dystrobrevin with the sarcoglycan sarcospan complex as a basis for understanding sarcoglycanopathy. Hum Mol Genet. 2000; 9:1033–40. [PubMed: 10767327]
21. Crawford GE, Faulkner JA, Crosbie RH, Campbell KP, Froehner SC, Chamberlain JS. Assembly of the dystrophin-associated protein complex does not require the dystrophin COOH-terminal domain. J Cell Biol. 2000; 150:1399–410. [PubMed: 10995444]
22. Yue Y, Liu M, Duan D. C-terminal-truncated microdystrophin recruits dystrobrevin and syntrophin to the dystrophin-associated glycoprotein complex and reduces muscular dystrophy in symptomatic utrophin/dystrophin double-knockout mice. Mol Ther. 2006; 14:79–87. [PubMed: 16563874]
23. Peters MF, Adams ME, Froehner SC. Differential association of syntrophin pairs with the dystrophin complex. J Cell Biol. 1997; 138:81–93. [PubMed: 9214383]
24. Brenman JE, Chao DS, Gee SH, McGee AW, Craven SE, Santillano DR, et al. Interaction of nitric oxide synthase with the postsynaptic density protein PSD-95 and alpha1-syntrophin mediated by PDZ domains. Cell. 1996; 84:757–67. [PubMed: 8625413]
25. Nawrotzki R, Loh NY, Ruegg MA, Davies KE, Blake DJ. Characterisation of alpha-dystrobrevin in muscle. J Cell Sci. 1998; 111:2595–605. [PubMed: 9701558]
26. Durbeej M, Cohn RD, Hrstka RF, Moore SA, Allamand V, Davidson BL, et al. Disruption of the beta-sarcoglycan gene reveals pathogenetic complexity of limb-girdle muscular dystrophy type 2E. Molecular cell. 2000; 5:141–51. [PubMed: 10678176]
27. Grady RM, Grange RW, Lau KS, Maimone MM, Nichol MC, Stull JT, et al. Role for alpha-dystrobrevin in the pathogenesis of dystrophin-dependent muscular dystrophies. Nat Cell Biol. 1999; 1:215–20. [PubMed: 10559919]
28. Yasuda S, Townsend D, Michele DE, Favre EG, Day SM, Metzger JM. Dystrophic heart failure blocked by membrane sealant poloxamer. Nature. 2005; 436:1025–9. [PubMed: 16025101]
29. Townsend D, Blankinship MJ, Allen JM, Gregorevic P, Chamberlain JS, Metzger JM. Systemic administration of micro-dystrophin restores cardiac geometry and prevents dobutamine-induced cardiac pump failure. Mol Ther. 2007; 15:1086–92. [PubMed: 17440445]

30. Schneider CA, Rasband WS, Eliceiri KW. NIH Image to ImageJ: 25 years of image analysis. Nature methods. 2012; 9:671–5. [PubMed: 22930834]
31. Coutu P, Bennett CN, Favre EG, Day SM, Metzger JM. Parvalbumin corrects slowed relaxation in adult cardiac myocytes expressing hypertrophic cardiomyopathy-linked alpha-tropomyosin mutations. Circ Res. 2004; 94:1235–41. [PubMed: 15059934]
32. Liu W, Ralston E. A new directionality tool for assessing microtubule pattern alterations. Cytoskeleton (Hoboken). 2014; 71:230–40. [PubMed: 24497496]
33. Johnson EK, Zhang L, Adams ME, Phillips A, Freitas MA, Froehner SC, et al. Proteomic analysis reveals new cardiac-specific dystrophin-associated proteins. PLoS One. 2012; 7:e43515. [PubMed: 22937058]
34. Petrof BJ, Shrager JB, Stedman HH, Kelly AM, Sweeney HL. Dystrophin protects the sarcolemma from stresses developed during muscle contraction. Proc Natl Acad Sci U S A. 1993; 90:3710–4. [PubMed: 8475120]
35. Khairallah RJ, Shi G, Sbrana F, Prosser BL, Borroto C, Mazaitis MJ, et al. Microtubules underlie dysfunction in duchenne muscular dystrophy. Sci Signal. 2012; 5:ra56. [PubMed: 22871609]
36. Percival JM, Gregorevic P, Odom GL, Banks GB, Chamberlain JS, Froehner SC. rAAV6-microdystrophin rescues aberrant Golgi complex organization in mdx skeletal muscles. Traffic. 2007; 8:1424–39. [PubMed: 17714427]
37. Prins KW, Humston JL, Mehta A, Tate V, Ralston E, Ervasti JM. Dystrophin is a microtubule-associated protein. J Cell Biol. 2009; 186:363–9. [PubMed: 19651889]
38. Prosser BL, Ward CW, Lederer WJ. X-ROS signaling: rapid mechano-chemo transduction in heart. Science. 2011; 333:1440–5. [PubMed: 21903813]
39. Townsend D, Yasuda S, McNally E, Metzger JM. Distinct pathophysiological mechanisms of cardiomyopathy in hearts lacking dystrophin or the sarcoglycan complex. Faseb J. 2011; 25:3106–14. [PubMed: 21665956]
40. Koo T, Malerba A, Athanasopoulos T, Trollet C, Boldrin L, Ferry A, et al. Delivery of AAV2/9-microdystrophin genes incorporating helix 1 of the coiled-coil motif in the C-terminal domain of dystrophin improves muscle pathology and restores the level of alpha1-syntrophin and alpha-dystrobrevin in skeletal muscles of mdx mice. Hum Gene Ther. 2011; 22:1379–88. [PubMed: 21453126]
41. Sharpe KM, Premsukh MD, Townsend D. Alterations of dystrophin-associated glycoproteins in the heart lacking dystrophin or dystrophin and utrophin. Journal of muscle research and cell motility. 2013; 34:395–405. [PubMed: 24096570]
42. Matsumura K, Ervasti JM, Ohlendieck K, Kahl SD, Campbell KP. Association of dystrophin-related protein with dystrophin-associated proteins in mdx mouse muscle. Nature. 1992; 360:588–91. [PubMed: 1461282]
43. Yang B, Ibraghimov-Beskrovnaya O, Moomaw CR, Slaughter CA, Campbell KP. Heterogeneity of the 59-kDa dystrophin-associated protein revealed by cDNA cloning and expression. J Biol Chem. 1994; 269:6040–4ff. [PubMed: 8119949]
44. Aquila-Pastir LA, DiPaola NR, Matteo RG, Smedira NG, McCarthy PM, Moravec CS. Quantitation and distribution of beta-tubulin in human cardiac myocytes. J Mol Cell Cardiol. 2002; 34:1513–23. [PubMed: 12431450]
45. Cerecedo D, Cisneros B, Mondragon R, Gonzalez S, Galvan IJ. Actin filaments and microtubule dual-granule transport in human adhered platelets: the role of alpha-dystrobrevins. Br J Haematol. 2010; 149:124–36. [PubMed: 20148881]
46. Mizuno Y, Thompson TG, Guyon JR, Lidov HG, Brosius M, Imamura M, et al. Desmuslin, an intermediate filament protein that interacts with alpha - dystrobrevin and desmin. Proc Natl Acad Sci U S A. 2001; 98:6156–61. [PubMed: 11353857]
47. Newey SE, Howman EV, Ponting CP, Benson MA, Nawrotzki R, Loh NY, et al. Syncoilin, a novel member of the intermediate filament superfamily that interacts with alpha-dystrobrevin in skeletal muscle. J Biol Chem. 2001; 276:6645–55. [PubMed: 11053421]
48. Harper SQ, Hauser MA, DelloRusso C, Duan D, Crawford RW, Phelps SF, et al. Modular flexibility of dystrophin: implications for gene therapy of Duchenne muscular dystrophy. Nat Med. 2002; 8:253–61. [PubMed: 11875496]

49. England SB, Nicholson LV, Johnson MA, Forrest SM, Love DR, Zubrzycka-Gaarn EE, et al. Very mild muscular dystrophy associated with the deletion of 46% of dystrophin. Nature. 1990; 343:180–2. [PubMed: 2404210]

50. Gregorevic P, Blankinship MJ, Allen JM, Crawford RW, Meuse L, Miller DG, et al. Systemic delivery of genes to striated muscles using adeno-associated viral vectors. Nat Med. 2004; 10:828–34. [PubMed: 15273747]

51. Lai Y, Thomas GD, Yue Y, Yang HT, Li D, Long C, et al. Dystrophins carrying spectrin-like repeats 16 and 17 anchor nNOS to the sarcolemma and enhance exercise performance in a mouse model of muscular dystrophy. J Clin Invest. 2009; 119:624–35. [PubMed: 19229108]

Highlights

- Isoproterenol challenge causes significant membrane damage in adbn$^{-/-}$ mice, despite the presence of full-length dystrophin.
- Dystrophin's interaction with dystrophin-glycoprotein complex is weakened in the absence of dystrobrevin.
- Hearts and cardiomyocytes are smaller in adbn$^{-/-}$ mice.
- Microtubule density and orientation is affected in adbn$^{-/-}$ mice.
- Together these findings have significant implications for the design of truncated dystrophins for gene therapy.

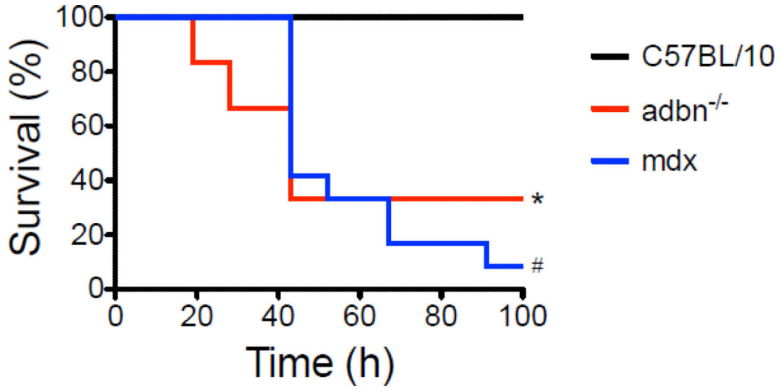

Figure 1. Chronic high dose isoproterenol challenge reveals heart insufficiency in adbn$^{-/-}$

Survival curves of C57BL/10 (n=9), adbn$^{-/-}$ (n=12) and mdx (n=12) mice subjected to a high-dose (30 mg/kg/day) isoproterenol test. Survival curves were generated using Kaplan-Meier method, Log-rank (Mantel-Cox) test was used to determine significant differences in survival from wild type; **P=0.0030: #P<0.0001*.

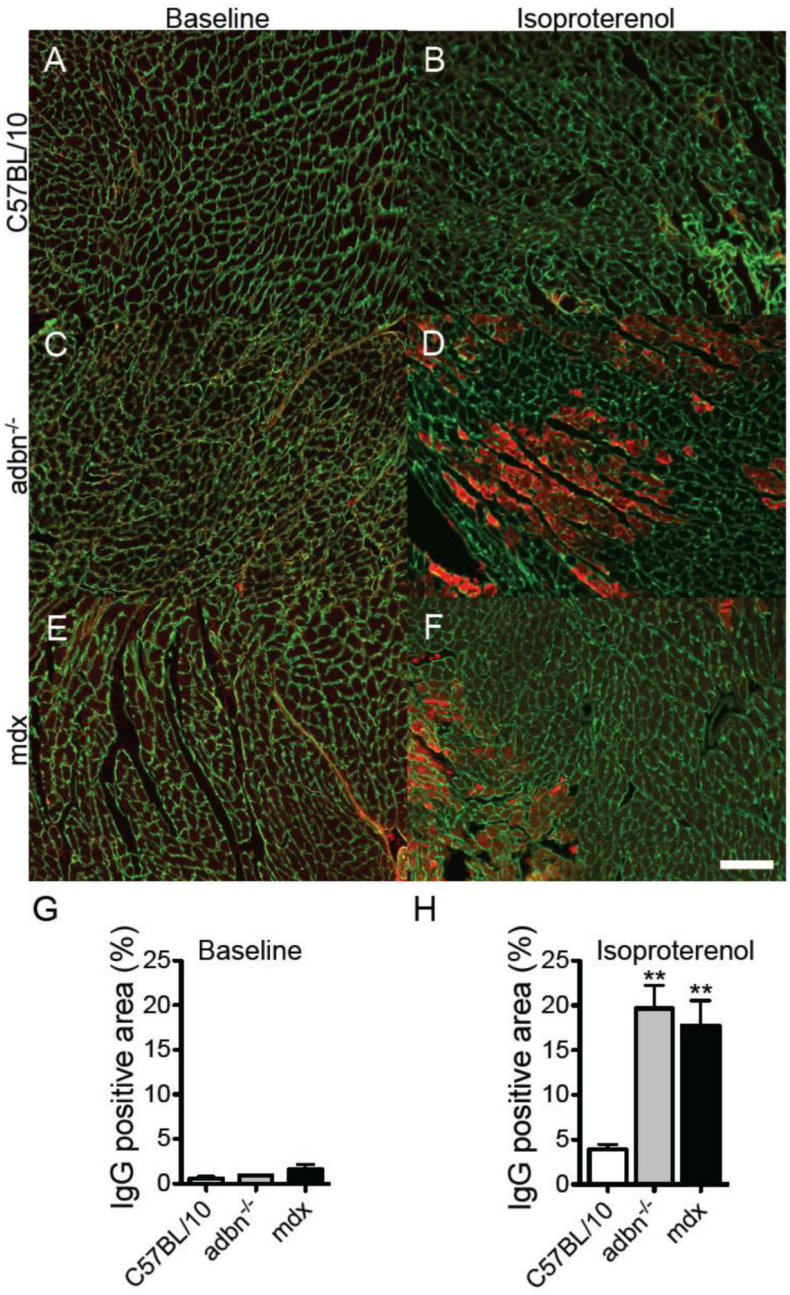

Figure 2. Increased IgG infiltration into dystrophic cardiac myocytes

(A-F) Representative heart sections/lesions from C57BL/10 (A.B). adbn$^{-/-}$ (CDI and mdx (E.F) mice at a baseline (A,C,E) or subjected to a high-dose isoproterenol test. Laminin is in green and IgG in red. The scales are equivalent and the bar represents 100 μm. (G,H) Quantification of myocardial injury as the amount of IgG infiltrated into cardiomyocytes at a baseline (G) and following isoproterenol test. Results are expressed relative to heart area. Results are presented as mean ± SEM (n=4-9); ***P<0.005* vs. C57BL/10.

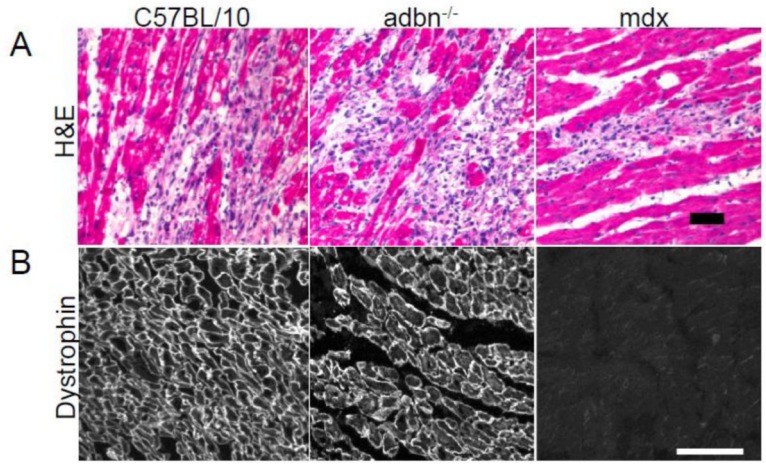

Figure 3. Histopatholoqical lesions and dystrophin expression in hearts following a high-dose isoproterenol challenge

(A) Representative heart sections from mice subjected to high-dose isoproterenol test (30 mg/kg/day) stained with hematoxylin and eosin (H&E) show development of scar tissue in C57BL/10. adbn$^{-/-}$, and mdx. Mice of each genotype that survived the longest are shown: C57BL/10 (120 h), adbn$^{-/-}$ (120 h). mdx (91 h). Bar represents 50 μm. (B) Representative images of heart sections from mice subjected to high dose isoproterenol test probed for dystrophin showing subcellular distribution of dystrophin in adbn$^{-/-}$ hearts is not different. Bar represents 100 μm.

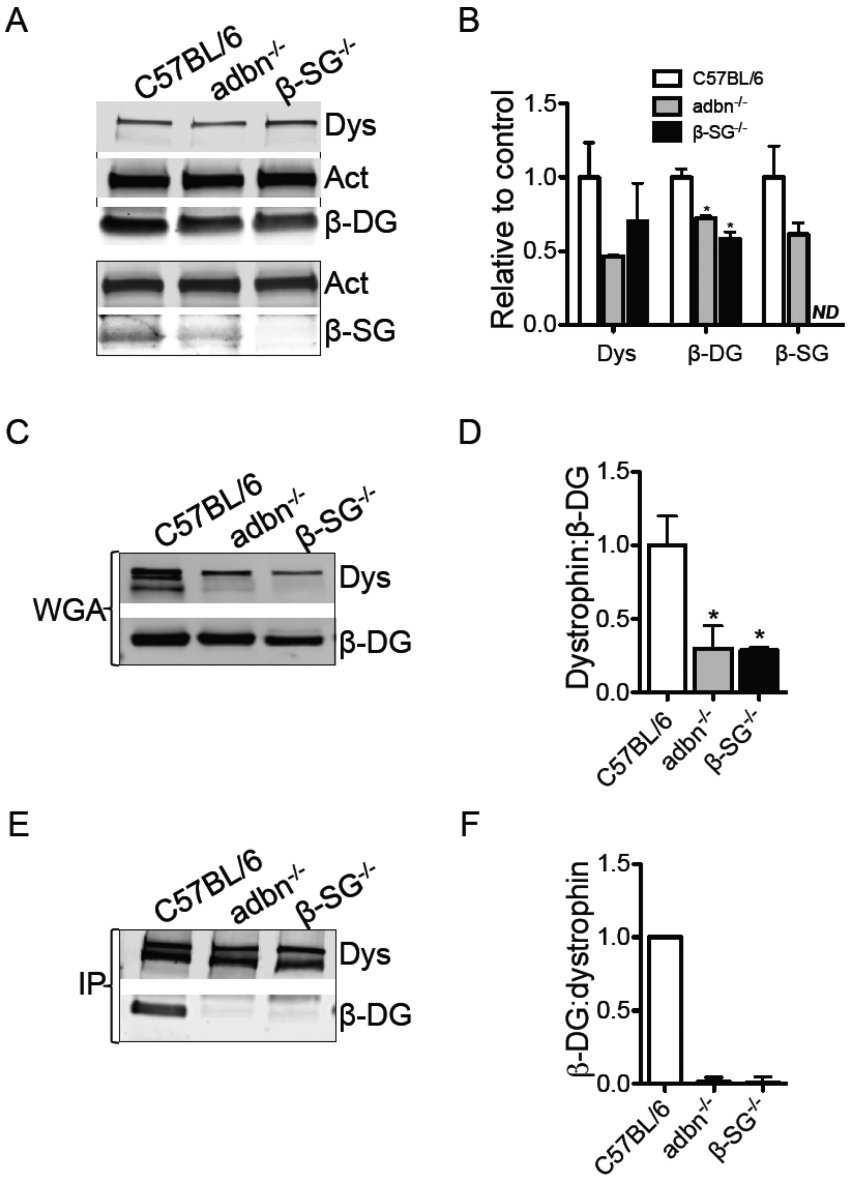

Figure 4. Alpha-dystrobrevin increases dystrophin binding to the membrane bound β-dystroqlycan

(A) Representative western blots showing the amount of dystrophin (Dys), β-dystrogvcan (β-DG) and β-sarcoqlycan (β-SG) in the heart homogenates from C57BU6. adbn$^{-/-}$ and β-sarcoalvcan (β-SG$^{-/-}$) mice. (B) Quantification of dystrophin. β-DG and β-SG. relative to α-actinin (n=3). (C) Representative western blot showing the amount of dystrophin and β-DG that was associated with wheat germ agglutinin (WGA). (D) Quantification of the dystrophin:β-DG ratio associated with WGA(n=4). (E) Immunoprecipitation (IP). Representative western blot showing the amount of dystrophin and β-DG that was pulled down an anti-dystrophin antibody. (F) Quantification of the β-DG:dystrophin ratio in the dystrophin IP (n=3). Results are presented as mean ± SEM, *$P<0.05$ vs. C57BL/6.

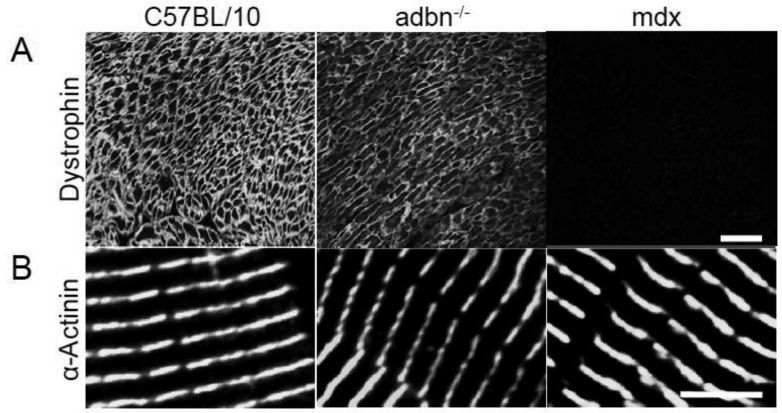

Figure 5. Adbrr$^{-/-}$ hearts have normal dystrophin localization and sarcomere pattern

(A) Representative heart sections showing dystrophin expression in untreated C57BL/10, adbn$^{-/-}$. and mdx hearts: n=3 per genotype: bar represents 100 μm; mixed gender. (B) Representative confocal images of primary cardiomyocytes showing expression of α-actinin in C57BL/10, adbn$^{-/-}$, and mdx mice; bar represents 5 μm; n=2 per genotype; 10 cells evaluated per genotype.

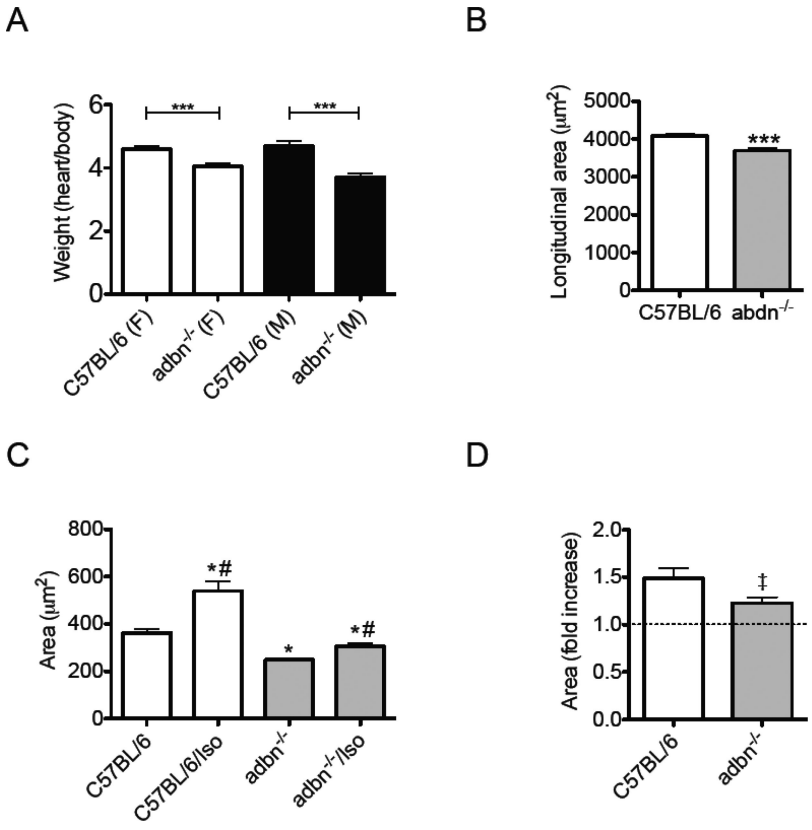

Figure 6. Adbn$^{-/-}$ cardiac myocytes have smaller cross-sectional area and have attenuated hypertrophy following chronic treatment with low-dose isoproterenol

(A)Heart to body weight ratio in C57BL/6 female (n=10) and male (n=10); adbn$^{-/-}$ female (n=6) and male (n=13) mice. (B) Longitudinal cell area (length × width) of cardiomyocytes isolated from C57BL/6 (n=4, 76-216 cells/heart) and adbn$^{-/-}$ (n=3, 81-170 cells/heart). (C) Quantification of cross-sectional area of in situ cardiomyocytes determined from laminin-stained heart sections from C57BL/6 (white) and adbn$^{-/-}$ (grey) mice. Saline and low-dose isoproterenol treatment groups are shown. (D) Shows the fold increase in the cross-sectional area of myocytes in hearts treated with low-dose isoproterenol-treated hearts relative to saline-treated controls. Data are presented as mean ± SEM, * signifies difference from saline treated C57BL/6 ($P<0.05$), # indicates a significant difference from saline treated adbn$^{-/-}$ ($P<0.05$), *”* denotes a significant difference between indicated pairs ($P<0.0001$), and ‡ demonstrates a significant difference from C57BL/6 ($P<0.05$).

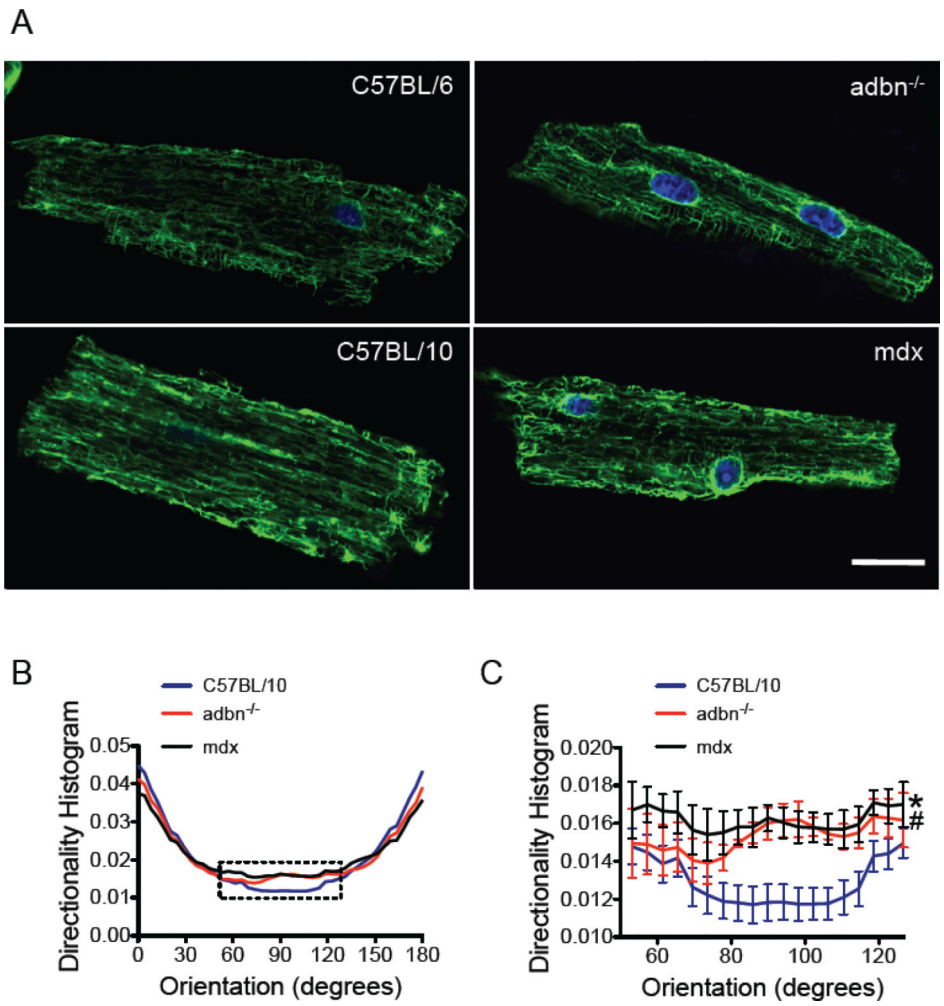

Figure 7. Microtubule directionality is affected in adbn$^{-/-}$ cardiomyocytes

(A) Representative confocal images of α-tubulin (green) immunofluorescence in cardiomyocytes (n≥3 mice with 10 cells/heart). DAPI is in blue. Bar represents 20 μm. (B) Microtubule orientation determined by TeDT analysis; 0° is defied as the longitudinal axis of the cell. Note that the error bars have been omitted to clarify the overall trends. The dashed lines indicate the area that is detailed in (C). (C) Magnification of the highlighted region of the orientation analysis shown in (B), with error bars, demonstrating the significantly increased prevalence of orthogonally directed microtubules in both mdx and adbn$^{-/-}$ myocytes (n≥3 mice with 10 cells/hearts). *Signifies difference between C57BL/10 and mdx. *P=0.0001* and #Signifies difference between C57BL/10 and adbn$^{-/-}$. *P<0.0001 by 2-way ANOVA.*

Table 1

Heart weight, body weight and cardiomyocyte dimensions.

	C57BL/6	*adbn*$^{-/-}$
Body weight females (g)	21.3 ± 0.3	22.7 ± 1.9
Heart weight females (mg)	98.0 ± 2.9	90.9 ± 5.9
Body weight males (g)	29.5 ± 0.6	35.6 ± 1.4**
Heart weight males (mg)	139.0 ± 6.8	130.7 ± 3.5
Cell width males (μm)	31.4 ± 0.4	29.6 ± 0.5**
Cell length males (μm)	130.3 ± 1.2	130.6 ± 1.5

Heart weight, body weight: C57BL/6 females (n=10), C57BL/6 males (n=10), adbn$^{-/-}$ females (n=6), adbn$^{-/-}$ males (n=13). Cell width and length: C57BL/6 male (n=4, 76-216 cells/heart) and adbn$^{-/-}$ males (n=3, 81-170 cells/heart). Data are expressed as mean ± SEM

** $P < 0.005$ vs. C57BL/6.